



ON THE EVAPORATION DYNAMICS OF ARRAY OF CYLINDRICAL AQUEOUS DROPLETS

Akam Aboubakri^{1,2}, Yigit Akkus³, Abdolali Sadaghiani^{1,2,*}, Khellil Sefiane⁴, Ali Koşar^{1,2,5,*}

¹ Faculty of Engineering and Natural Sciences (FENS), Sabanci University, Orhanli, 34956, Tuzla, Istanbul, Turkey

² Sabanci University Nanotechnology and Application Center (SUNUM), Sabanci University, Orhanli, 34956, Tuzla, Istanbul, Turkey

³ ASELSAN Inc., 06200, Yenimahalle, Ankara, Turkey

⁴ School of Engineering, University of Edinburgh, Edinburgh EH8 9YL, UK

⁵ Center of Excellence for Functional Surfaces and Interfaces for Nano-Diagnostics (EFSUN), Sabanci University, Orhanli, 34956, Tuzla, Istanbul, Turkey

ABSTRACT

Droplet evaporation, as one of the most observed phenomena in nature, plays important roles in many applications, namely droplet-based biosensors, spray cooling, and inkjet printing, among others. The evaporation dynamics of a single droplet has been widely studied. However, the literature lacks enough studies investigating the effect of collective behaviour of droplets, which necessarily should be considered in many applications. In this study, based on a previously developed algorithm, we have studied the effect of adjacency of droplets on the velocity field of adjacent cylindrical droplets. Based on the obtained results, at the presence of thermocapillary effect, in both central and side droplets two separate flows are found. At the absence of the thermocapillary effect, the central droplet has two possible scenarios: outward capillary flow, and presence of two separate buoyancy induced circulations. Moreover, at the side droplet there are three possible scenarios. First, the capillary flow overweighs the buoyancy flow; second, one circulation is observed in the liquid domain; and finally, two separate buoyancy induced flows are seen. According to the obtained results, the velocity field in all the cases is dependant of droplet pitch size (distance between the droplets), superheat temperature (temperature difference between surface and environment), and droplet diameter. At the last step, the effect of the obtained velocity field on the temperature field is discussed.

1. INTRODUCTION

Droplet evaporation plays a key role in many industrial applications from material science and crystallization to bioscience and thermal management [1]. During evaporation of the droplet, the fluid flows at both liquid and gas phases. In the liquid phase there are three flows; first a flow from the interface to the contact line, known as capillary flow [2]; second buoyancy driven flow which stems from density gradient inside the droplet [3]; and the third one is a flow which arises from surface tension gradient [4]. On the other hand, there are two coexisting flows at the gas phase: natural convection [5] and Stefan flow [6], which originate from density and vapor concentration gradient, respectively. The combination of these flows strongly affects the evaporation dynamics of the droplet and resulted outcome [7]. Evaporation dynamics of a single droplet is investigated intensively in the literature both experimentally and numerically [5]. However, the neighbouring droplets strongly affect the velocity and temperature field inside each other [8]. Not many studies have dealt with the collective behaviour of droplets in the literature. Pradhan et al. [9] investigated the effect of neighbouring binary droplets on the buoyant flow each droplet. They reported that both droplets tend to show behavior of a single droplet with increment in the distance between the droplets. In another study, Basu et al. [10] studied self-assembly of adjacent droplets and found a cavity on the neighboring side of each droplet.

The literature lacks a study which analyzes the effect of different parameters on adjacent droplets. In this study, a developed algorithm developed by Akkus et al [4] is used for numerical simulation of three adjacent droplets. Here, we present the changes in the velocity fields in both liquid and gas domains

*Corresponding Author: a.sadaghiani@sabanciuniv.edu

and the resultant temperature fields are investigated. The studied parameters are distance between the droplets, superheat temperature, and droplet diameter.

2. NUMERICAL ANALYSIS

2.1 Governing equations

In order to simulate the evaporation of droplet, the conservation of mass, momentum, and energy should be solved in both liquid and gas phase. Moreover, the gas phase requires convective and diffusive vapor transport equation to obtain the evaporation rate. These equations are presented as follows:

$$\nabla \cdot (\rho \mathbf{u}) = 0 \quad (1)$$

$$\rho(\mathbf{u} \cdot \nabla) \mathbf{u} = \rho \mathbf{g} - \nabla p + \mu \nabla^2 \mathbf{u} \quad (2)$$

$$\mathbf{u} \cdot \nabla T = \alpha (\nabla^2 T) + \Phi \quad (3)$$

$$-\mathbf{u} \cdot \nabla C_v + \nabla \cdot (D_{w-air} \nabla C_v) = 0 \quad (4)$$

where ρ and \mathbf{u} are the density of the fluid, velocity vector. Moreover, \mathbf{g} , p , μ , T , and C_v represent gravitational acceleration, pressure, viscosity of the fluid, temperature, and vapor concentration, respectively. Furthermore D_{w-air} is the temperature dependent diffusivity constant of water vapor and air [11]. Moreover, α represents the thermal diffusivity of the fluid, and Φ is the viscous dissipation term. To simulate the natural convection in both of gas and liquid phases, weakly compressible approach is considered in the model. Since the velocities are relatively low and the size of the geometry is small, the flow of both phases is considered to be laminar.

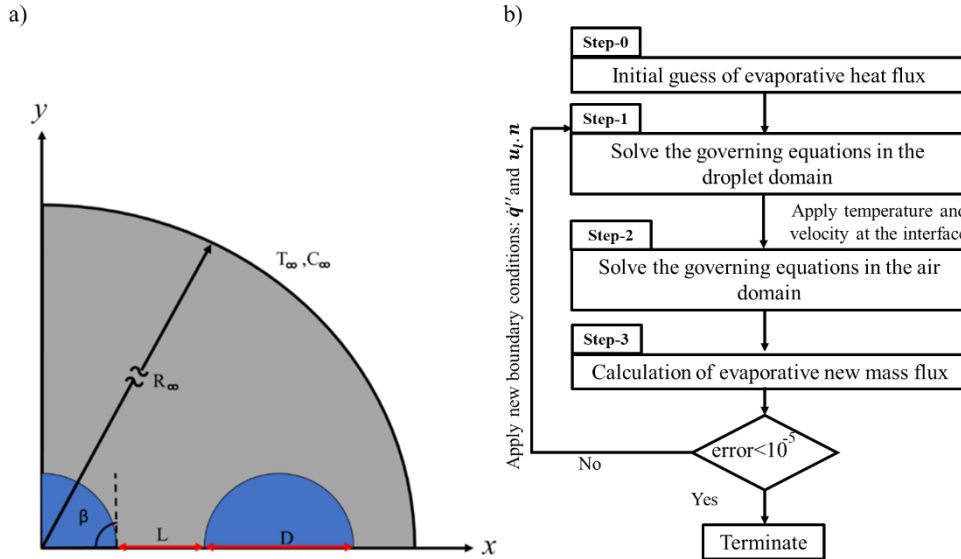


Figure 1: a) Schematic figure of computational domain b) Algorithm flow chart of the interface boundary condition

2.1 Boundary conditions

In the simulations, the gas and liquid phases are simulated separately. However, an iterative algorithm, developed by Akkus et al. [4] is used at the interface (see Fig. 1b). The other boundary conditions can be summarized as follows:

(I). At the x-axis, non-slip boundary condition is used for equations (1) and (2). Moreover, constant temperature is used as thermal boundary condition. Finally, equation (4) requires no-vapor penetration, considering the solid surface placed under the droplet.

(II). At the y-axis, a symmetric boundary condition is applied to all equations.

(III). The outer boundaries are considered to be much larger than the size of droplet, to enable the model to simulate natural convection at the gas domain. At outer boundary, ambient temperature, pressure, and relative humidity is used to the model.

3. RESULT AND DISCUSSION

Fig. 2 shows the interfacial temperature distribution at the interface of both central and side droplets with different diameters at non-dimensional pitch size of $L/D=0.5$. Accordingly, the interfacial temperature of both central and side droplets decreases with increment in diameter. This is due to

increase in the thermal resistance with droplet diameter. However, at the absence of thermocapillary flow (Fig. 2b), the variation in the interfacial temperature is more complicated. At the central droplet, while the diameter of the droplet is smaller than 4mm, the interfacial temperature decreases with diameter. For droplet with $D=5\text{mm}$, the buoyancy strongly affects the interfacial temperature. At the side droplet, while the diameter is smaller than 3mm, the interfacial temperature is not affected by buoyancy flow. On the other hand, for droplets with diameters larger than 4mm, the buoyancy driven flow strongly affect the interfacial temperature distribution.

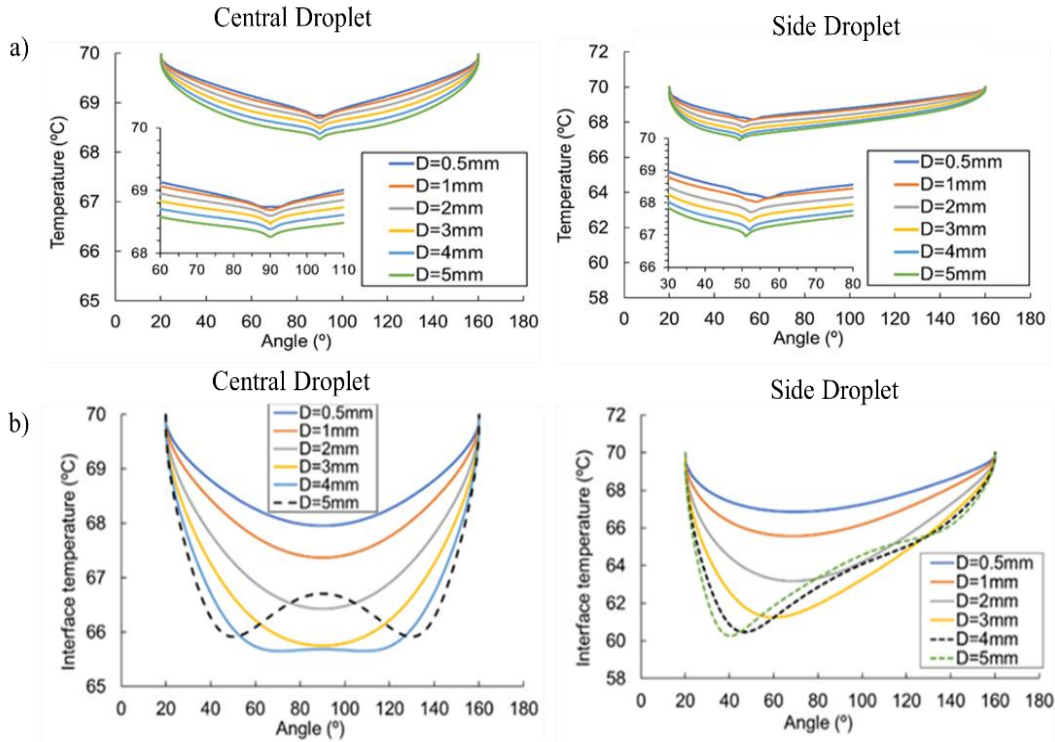


Figure 2: Interfacial temperature distribution a) with thermocapillary effect b) without thermocapillary effect

Figure 3 shows the predicted evaporative heat fluxes of the evaporating droplet. Compared to their central pair, all side droplets have larger evaporative heat fluxes. As seen in Fig. 3a, in the presence of thermocapillary flow, a sudden decrease in the evaporative heat flux is found. This sudden decrease lessens with increase in the diameter. As their interfacial temperature, droplets with larger diameters have a smaller evaporative heat flux, due to increase in thermal resistance. Moreover, the evaporative heat flux of the side droplet is larger than the central droplet. On the other hand, at the absence of thermocapillary effect (Fig. 3b), while the buoyancy flow is strong enough to change the interfacial temperature distribution, the evaporative heat flux increases as well.

4. CONCLUSIONS

The effect of drop adjacency on droplet evaporation plays a vital role in wide range of applications from spray cooling to microfluidics and inject printings. By developing a fully coupled numerical approach the effects of droplet adjacency on evaporation dynamics of aqueous cylindrical droplets were investigated in this work. Using non-dimensional droplet pitch distance (L/D), the interfacial temperature and distributed heat flux at the interface of the cylindrical droplets are investigated. In the absence of Marangoni flow, the outermost droplet has a higher evaporation rate than the central one. However, in the presence of Marangoni flow, when the non-dimensional pitch size is larger than 5 ($L/D > 5$), there are two possible scenarios as (i) at low superheat temperatures ($\Delta T < 30^\circ\text{C}$), the outer droplet has an evaporation rate higher than the central one; (ii) at high superheat temperatures ($\Delta T > 30^\circ\text{C}$ which corresponds to high droplet Rayleigh numbers), the evaporation rate of the outer droplet is lower than the central droplet.

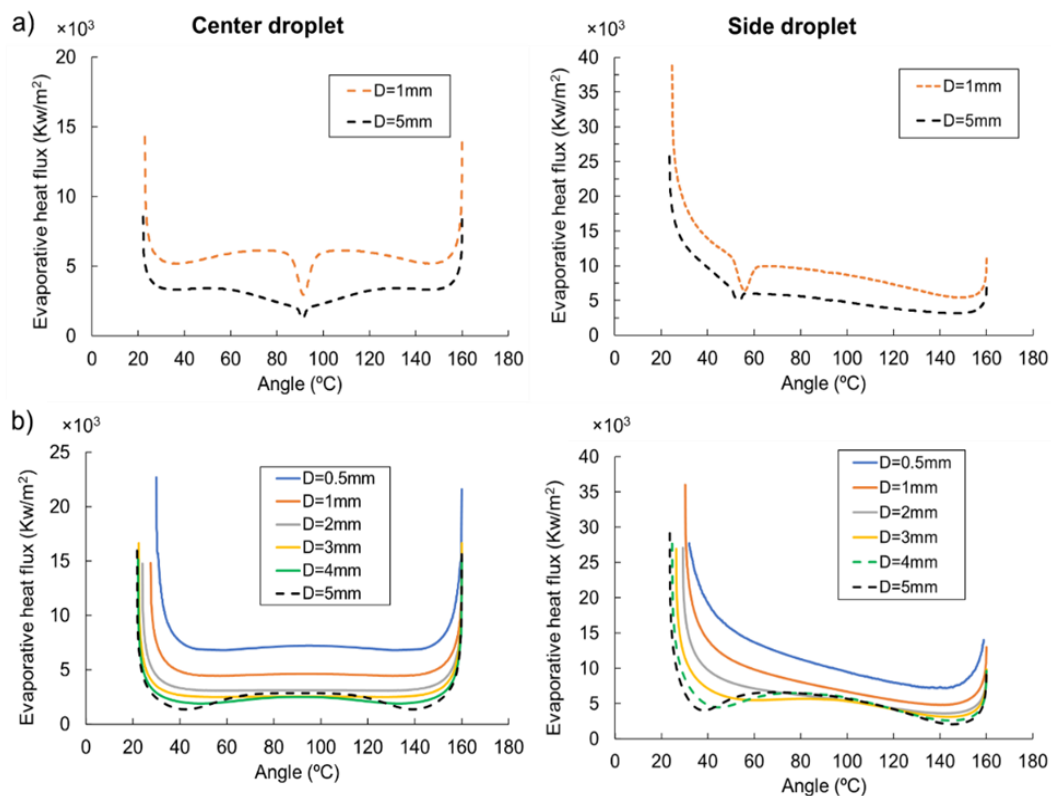


Figure 3: Evaporative heat flux a) with thermocapillary effect b) without thermocapillary effect

REFERENCES

1. Zang, D., et al., *Evaporation of a Droplet: From physics to applications*. Physics Reports, 2019. **804**: p. 1-56.
2. Wu, Z., et al., *Surface-tension-confined assembly of a metal–organic framework in femtoliter droplet arrays*. RSC advances, 2018. **8**(7): p. 3680-3686.
3. Kang, K.H., et al., *Evaporation-induced saline Rayleigh convection inside a colloidal droplet*. Physics of Fluids, 2013. **25**(4): p. 042001.
4. Akkus, Y., B. Cetin, and Z. Dursunkaya, *A theoretical framework for comprehensive modeling of steadily fed evaporating droplets and the validity of common assumptions*. International Journal of Thermal Sciences, 2020. **158**: p. 106529.
5. Aboubakri, A., et al. *Numerical and Experimental Investigation on Evaporation of Water Droplet on Surfaces With Mixed Wettability*. in *ASME 2020 18th ICNMM collocated with the ASME 2020 Heat Transfer Summer Conference and the ASME 2020 Fluids Engineering Division Summer Meeting*. 2020. American Society of Mechanical Engineers Digital Collection.
6. Akkus, Y., *THE EFFECT OF STEFAN FLOW ON THE MODELS OF DROPLET EVAPORATION*. Isı Bilimi ve Tekniği Dergisi, 2020. **40**(2): p. 309-318.
7. Wang, J., et al., *Patterned photonic crystals fabricated by inkjet printing*. Journal of Materials Chemistry C, 2013. **1**(38): p. 6048-6058.
8. Shaikeea, A.J.D. and S. Basu, *Insight into the evaporation dynamics of a pair of sessile droplets on a hydrophobic substrate*. Langmuir, 2016. **32**(5): p. 1309-1318.
9. Pradhan, T.K. and P.K. Panigrahi, *Influence of an adjacent droplet on fluid convection inside an evaporating droplet of binary mixture*. Colloids and Surfaces A: Physicochemical and Engineering Aspects, 2016. **500**: p. 154-165.
10. Shaikeea, A., et al., *Insights into vapor-mediated interactions in a nanocolloidal droplet system: evaporation dynamics and affects on self-assembly topologies on macro-to microscales*. Langmuir, 2016. **32**(40): p. 10334-10343.
11. Bolz, R.E., *CRC handbook of tables for applied engineering science*. 1973: CRC press.